JOURNAL OF GUIDANCE, CONTROL, AND DYNAMICS
Vol. 20, No. 2, March–April 1997

Optimal Earth–Moon Trajectories Using Combined Chemical–Electric Propulsion

Craig A. Kluever*
University of Missouri–Columbia/Kansas City, Kansas City, Missouri 64110-2499

Minimum-fuel, three-dimensional Earth–moon trajectories are obtained for spacecraft using both chemical and electric propulsion stages. The problem involves maximizing the final spacecraft mass delivered to a circular, polar midlunar orbit. The mission definition involves a chemical-stage boost from low-Earth orbit into a coasting ballistic trajectory followed by a lunar capture trajectory performed by the electric propulsion stage. For this analysis, the ballistic orbit transfer and the powered orbit transfer to a circular orbit within the lunar sphere of influence are modeled by the dynamics of the classical restricted three-body problem, and two body-centered coordinate frames are utilized. The subsequent descending three-dimensional spiral trajectory to circular polar midlunar orbit is computed via Edelbaum's analytic equations in order to eliminate the need to numerically simulate the numerous near-circular lunar orbits. Two classes of current-term electric propulsion thrusters are utilized (arcjet and plasma thrusters) along with current-term launch vehicle configurations. Numerical results are presented, and the optimal chemical–electric propulsion transfers exhibit a substantial reduction in trip time compared to Earth–moon transfers using electric propulsion alone.

Introduction

LOW-THRUST trajectory optimization has been a popular research topic in recent years.[1–3] The practical appeal of low-thrust electric propulsion (EP) involves the improved payload mass ratio in comparison to conventional chemical propulsion systems. However, this payload enhancement is usually at the cost of a substantial increase in total trip time. In particular, the payload enhancement for an orbit transfer from low Earth orbit (LEO) to geosynchronous orbit (GEO) using EP has been well documented.[4,5] However, this maneuver is currently a far-term application of electric propulsion. A projected near-term benefit of low-thrust propulsion involves the combination of conventional chemical propulsion with EP for the LEO–GEO orbit transfer.[6,7]

Among the numerous mission applications of electric propulsion, the minimum-fuel low-thrust transfer from LEO to low lunar orbit (LLO) has been investigated by various researchers.[8–11] The minimum-fuel, low-thrust LEO–LLO transfer usually involves several near-circular, powered, spiral orbits about the Earth and moon connected by a translunar arc. Consequently, the use of low-thrust propulsion alone can require several months to complete the LEO–LLO transfer. In addition, a slowly unwinding Earth-escape spiral trajectory will spend a great deal of time within the Van Allen radiation belts, which can result in substantial power degradation for solar electric propulsion (SEP) vehicles using solar arrays.

Unlike the LEO–GEO application, the combined use of chemical and electric propulsion stages for the Earth–moon orbit transfer has not been investigated in detail. A preliminary analysis of mission and spacecraft optimization was performed for a chemical–EP spacecraft for a lunar-interplanetary mission but the trajectory optimization techniques utilized completely analytic approximations for the low-thrust orbit transfers.[12] In this paper, we obtain optimal minimum-fuel trajectories for a three-dimensional, Earth–moon, orbit transfer using both chemical and EP stages. The mission definition involves a chemical-stage boost from LEO into a coasting translunar trajectory followed by a lunar capture into a 4000-km altitude circular polar midlunar orbit (MLO) performed by the EP stage. For this analysis, the translunar trajectory [beginning in LEO and terminating within the lunar sphere of influence (SOI)] is modeled by the dynamics of the classical restricted three-body problem, and analytic methods are utilized for the three-dimensional powered transfer to the circular polar MLO. Two classes of EP modes, namely, arcjet thrusters and stationary plasma thrusters (SPT), are investigated and numerical results are presented.

Received June 10, 1996; presented as Paper 96-3650 at the AIAA/AAS Astrodynamics Specialist Conference, San Diego, CA, July 29–31, 1996; revision received Nov. 18, 1996; accepted for publication Nov. 25, 1996.

*Assistant Professor, Mechanical and Aerospace Engineering. Member AIAA.

System Models

Ballistic Coasting Trajectory

As previously mentioned, the translunar trajectory is governed by the classical restricted three-body problem dynamics.[13] Because the orbit transfer consists of two distinct phases (a coasting ballistic trajectory and a powered low-thrust capture trajectory) with boundary conditions in the vicinity of both primary bodies, two body-centered coordinate frames are utilized. The three-dimensional equations of motion for the coasting spacecraft during the ballistic translunar trajectory are presented in an Earth-centered, rotating, Cartesian frame:

$$\frac{dx}{dt} = u \tag{1}$$

$$\frac{dy}{dt} = v \tag{2}$$

$$\frac{dz}{dt} = w \tag{3}$$

$$\frac{du}{dt} = -\frac{\mu_1 x}{\rho_1^3} + \frac{\mu_2 (D - x)}{\rho_2^3} - \frac{\mu_2}{D^2} + 2\omega v + \omega^2 x \tag{4}$$

$$\frac{dv}{dt} = -\frac{\mu_1 y}{\rho_1^3} - \frac{\mu_2 y}{\rho_2^3} - 2\omega u + \omega^2 y \tag{5}$$

$$\frac{dw}{dt} = -\frac{\mu_1 z}{\rho_1^3} - \frac{\mu_2 z}{\rho_2^3} \tag{6}$$

The rotating Cartesian frame's origin is the Earth's center with the positive x axis pointing to the moon's center along the Earth–moon line. The y axis is in the Earth–moon orbit plane, and the positive z axis is along the angular momentum vector of the Earth–moon system. The position and velocity components of the spacecraft with respect to the Earth's center are denoted by x, y, z and u, v, w, and radial distances from the Earth and moon are denoted by ρ_1 and ρ_2, respectively. As defined by the restricted three-body problem, the Earth and moon are assumed to revolve in circular orbits about their common center of mass. The gravitational parameters of the Earth and moon are denoted by μ_1 and μ_2, the constant Earth–moon

separation distance is D, and the constant Earth–moon system angular rate is ω.

Initially, the spacecraft is injected into a ballistic translunar trajectory from LEO by the upper stage of a Taurus launch vehicle. The spacecraft injection point in LEO with respect to the Earth-centered rotating frame is

$$x(0) = \rho_1(0)(\cos\Omega_0\cos\theta_0 - \sin\Omega_0\sin\theta_0\cos i_0) \tag{7}$$

$$y(0) = \rho_1(0)(\sin\Omega_0\cos\theta_0 + \cos\Omega_0\sin\theta_0\cos i_0) \tag{8}$$

$$z(0) = \rho_1(0)\sin\theta_0\sin i_0 \tag{9}$$

where Ω_0 is the argument of the ascending node, θ_0 is the longitude angle, and i_0 is inclination. Ascending node angle Ω_0 is measured from an inertial x–axis direction to the line of nodes in the x–y plane. At the injection point, the $+x$ axis of the inertial frame is aligned with the rotating frame and, therefore, points toward the moon. Longitude angle θ_0 is measured from the ascending node to the spacecraft in the orbit plane. For our preliminary analysis, inclination i_0 is assumed to be fixed at 7 deg, which represents the difference between the LEO plane and the Earth–moon orbit plane for a launch in 2000. The initial radius $\rho_1(0)$ is 6563.1 km, which corresponds to LEO for a Taurus launch vehicle.

The initial velocity components of the spacecraft in the Earth-centered rotating frame after translunar injection (TLI) are

$$u(0) = -v_{\text{bo}}(\cos\Omega_0\sin\theta_0 + \sin\Omega_0\cos\theta_0\cos i_0) + \omega y(0) \tag{10}$$

$$v(0) = -v_{\text{bo}}(\sin\Omega_0\sin\theta_0 - \cos\Omega_0\cos\theta_0\cos i_0) - \omega x(0) \tag{11}$$

$$w(0) = v_{\text{bo}}\cos\theta_0\sin i_0 \tag{12}$$

where v_{bo} is the translunar injection velocity after burnout of the Taurus upper stage as defined by

$$v_{\text{bo}} = \left(C_3 + \frac{2\mu_1}{\rho_1(0)}\right)^{\frac{1}{2}} \tag{13}$$

where C_3 is the injection energy.

Low-Thrust Capture Trajectory

The low-thrust, powered, capture trajectory is governed by the three-body problem dynamics formulated in a moon-centered, inertial, orbit-plane frame

$$\frac{\mathrm{d}r}{\mathrm{d}t} = v_r \tag{14}$$

$$\frac{\mathrm{d}v_r}{\mathrm{d}t} = \frac{v_\theta^2}{r} + \frac{T}{m}\alpha_r + \nabla U_r \tag{15}$$

$$\frac{\mathrm{d}v_\theta}{\mathrm{d}t} = -\frac{v_r v_\theta}{r} + \frac{T}{m}\alpha_\theta + \nabla U_\theta \tag{16}$$

$$\frac{\mathrm{d}\Omega}{\mathrm{d}t} = \frac{\sin\theta}{v_\theta\sin i}\left(\frac{T}{m}\alpha_h + \nabla U_h\right) \tag{17}$$

$$\frac{\mathrm{d}i}{\mathrm{d}t} = \frac{\cos\theta}{v_\theta}\left(\frac{T}{m}\alpha_h + \nabla U_h\right) \tag{18}$$

$$\frac{\mathrm{d}\theta}{\mathrm{d}t} = \frac{v_\theta}{r} - \frac{\sin\theta\cos i}{v_\theta\sin i}\left(\frac{T}{m}\alpha_h + \nabla U_h\right) \tag{19}$$

$$\frac{\mathrm{d}m}{\mathrm{d}t} = -\beta \tag{20}$$

Here, the states of the system are radial position r, radial velocity v_r, transverse velocity v_θ, ascending node angle Ω, inclination i, longitude θ, and spacecraft mass m. The $+x$ axis of the moon-centered inertial frame points from the moon center to the Earth at the instant the low-thrust capture trajectory is initiated. As before, ascending node Ω is measured from the $+x$ axis in the Earth–moon (x–y) plane, inclination is measured from the normal of the x–y plane, and θ is measured in the orbit plane from the ascending node to the spacecraft. Propulsive thrust is denoted by T, and mass flow rate is β. The thrust acceleration direction is determined by the three-direction cosine components, $\boldsymbol{\alpha} = [\alpha_r, \alpha_\theta, \alpha_h]^T$, which are projections of the thrust vector along a rotating radial frame (the RTH frame) defined by the unit vector $\boldsymbol{i} = [\boldsymbol{i}_r, \boldsymbol{i}_\theta, \boldsymbol{i}_h]^T$,

$$\boldsymbol{i}_r = \frac{\boldsymbol{r}}{\|\boldsymbol{r}\|} \tag{21}$$

$$\boldsymbol{i}_h = \frac{\boldsymbol{r}\times\boldsymbol{v}}{\|\boldsymbol{r}\times\boldsymbol{v}\|} \tag{22}$$

$$\boldsymbol{i}_\theta = \boldsymbol{i}_h \times \boldsymbol{i}_r \tag{23}$$

where $\boldsymbol{r}$ and $\boldsymbol{v}$ denote the spacecraft's position and velocity in the moon-centered coordinate frame.

Finally, U is the two-body gravity potential of the Earth and moon and its gradient is

$$\nabla U = -\left(\mu_2\boldsymbol{r}/r^3\right) - \mu_1\left[\left(\boldsymbol{r}_1/r_1^3\right) - \left(\boldsymbol{r}_{12}/D^3\right)\right] \tag{24}$$

where $\boldsymbol{r}_1$ is the Earth-spacecraft position vector and $\boldsymbol{r}_{12}$ is the Earth-moon position vector. The calculation of these position vectors in the moon-centered RTH frame is described in detail in Appendix A.

Low-Thrust Quasicircular Transfer

Typically, low-thrust transfers require hundreds of tight, near-circular orbits during the final phase of the powered transfer to the desired circular orbit. Numerical simulation of these near-circular orbits requires thousands of integration steps and would, therefore, greatly increase the computational cost of the problem. To improve convergence properties and reduce the computational load, the fuel consumed during these slowly descending, near-circular, spiral trajectories to polar MLO are approximated by analytical equations developed by Edelbaum[14] for minimum-fuel, low-thrust, transfer problems between inclined circular orbits. Edelbaum's expression for a low-thrust circle-to-circle (quasicircular) transfer with plane change is the rocket equation

$$\frac{m(t_F)}{m(t_f)} = \exp\left(\frac{-\Delta V}{g I_{\text{sp}}}\right) \tag{25}$$

where $m(t_f)$ is the final mass at the end of the numerically simulated powered lunar capture (the initial mass for the start of the quasicircular transfer) and $m(t_F)$ is the final mass in polar MLO. In Eq. (25), I_{sp} is specific impulse and g is the Earth's gravitational acceleration at sea level. The variable ΔV is the velocity increment between inclined circular orbits and includes the velocity required for a plane change. Edelbaum's expression for ΔV is

$$\Delta V^2 = V_1^2 + V_2^2 - 2V_1V_2\cos(\pi\Delta i/2) \tag{26}$$

where V_1 and V_2 are the initial and final circular velocities and Δi is the plane change in degrees between the circular orbits. Therefore, the spacecraft mass in MLO is

$$m_{\text{MLO}} = m(t_F) = m(t_f)\exp(-\Delta V/g I_{\text{sp}}) \tag{27}$$

The corresponding quasicircular transfer time Δt_{QC} is

$$\Delta t_{\text{QC}} = \frac{m(t_f) - m(t_F)}{\beta} \tag{28}$$

Therefore, the final end time in polar MLO is $t_F = t_f + \Delta t_{\text{QC}}$.

Spacecraft System Models

The lunar probe is injected into a translunar ballistic trajectory by the upper stage of a Taurus launch vehicle. The injected mass m_{TLI} is computed by a simple linear fit of the launch performance,

$$m_{\text{TLI}} = m_{C_3}C_3 + m_0 \tag{29}$$

where m_{C_3} is the mass change with respect to C_3 and m_0 is the injected mass for escape conditions with zero hyperbolic excess

Table 1 Taurus launch vehicle performance constants

Configuration	m_{C_3}, kg-s^2/km^2	m_0, kg
SRMs	−10	380
No SRMs	−6.2	330

Table 2 Electric propulsion system parameters

Thruster	P, W	I_{sp}, s	η	β, kg/day
Arcjet	800	450	0.32	2.27
SPT	700	1600	0.46	0.23

energy ($C_3 = 0$). Taurus launch vehicle configurations with and without strap-on solid rocket motors (SRMs) are utilized, and the corresponding constants for launch performance are shown in Table 1 (Ref. 15). The two different Taurus configurations were utilized so that the cheapest launch option for delivering a spacecraft in excess of 300 kg to MLO could be identified.

The powered lunar capture maneuver is performed by the SEP stage. Propulsive force is determined by

$$T = 2\eta P/c \tag{30}$$

where P is the input power to the thrusters, η is the thruster efficiency, and c is the engine exhaust velocity. The exhaust velocity is

$$c = I_{sp}g \tag{31}$$

It is assumed that P, η, and I_{sp} remain constant, which implies a constant thrust magnitude and no engine throttling. Finally, mass flow rate is determined by

$$\beta = T/c \tag{32}$$

Two different commercially available EP thrusters are investigated, namely, arcjet thrusters and SPT. The system parameters utilized in this analysis are presented in Table 2, and these values represent the current level in EP technology.[16]

Trajectory Optimization

Problem Statement

The objective is to compute the minimum-fuel transfer from LEO to polar MLO using an impulsive chemical burn at LEO followed by a continuous-thrust lunar capture performed by the SEP stage. The complete optimal control problem is given as follows.

For the free end-time problem, find the optimal injection energy C_3; the angles Ω_0 and θ_0, which define the position of the spacecraft at TLI; the ballistic coast time t_{coast}; the thrust acceleration direction cosines $\boldsymbol{\alpha}(t)$; and the powered SEP capture time t_{capt}, which minimize

$$J = -m(t_F) = -m_{MLO} \tag{33}$$

subject to the unpowered equations of motion (1–6) for $0 \le t \le t_{coast}$ with the initial conditions (7–13), and subject to the powered equations of motion (14–20) with the terminal state constraints

$$\boldsymbol{\Psi}[\boldsymbol{x}(t_f), t_f] = \begin{pmatrix} v_r(t_f) \\ v_\theta(t_f) - \sqrt{\mu_2/r} \end{pmatrix} = \begin{pmatrix} 0 \\ 0 \end{pmatrix} \tag{34}$$

and the inequality constraint, in kilometers,

$$r(t_f) \le 66{,}300 \tag{35}$$

and subject to the powered quasicircular transfer equation to polar MLO indicated by Eqs. (25) and (26).

The motion of the spacecraft is governed by the two sets of differential equations (1–6) and (14–20). Initial conditions for the powered equations of motion (14–20) are obtained by transforming the end conditions of the unpowered ballistic trajectory at $t = t_{coast}$ to the inertial moon-centered frame. The details of this transformation are presented in Appendix B. The terminal state constraints (34) and inequality constraint (35) require that the numerically simulated powered lunar capture trajectory terminate in a circular lunar orbit with an altitude below the lunar SOI. Furthermore, the subsequent quasicircular transfer from this circular high lunar orbit of arbitrary inclination to the polar MLO is computed via Edelbaum's[14] approximation presented by Eqs. (25) and (26). This quasicircular approximation is used to compute the final spacecraft mass m_{MLO} at $t = t_F$. Again, the purpose of this approximation is to remove the necessity to numerically integrate hundreds of near-circular orbits about the moon during the transfer to polar MLO.

Solution Method

Because the optimal control problem involves a mix of continuous control functions [the thrust direction cosines $\boldsymbol{\alpha}(t)$] and discrete control parameters (initial orbit angles, launch energy, and coast/burn times) the problem is solved using a direct method. In particular, the optimal control problem is replaced by a nonlinear programming (NLP) problem, which in turn is numerically solved by a constrained parameter optimization method, namely, sequential quadratic programming (SQP).[17] The SQP algorithm used here utilizes finite differences to approximate the gradients and was developed by Pouliot.[18]

To avoid ambiguities in the thrust vector direction, the three-direction cosines $\boldsymbol{\alpha}(t) = [\alpha_r, \alpha_\theta, \alpha_h]^T$ are utilized as the continuous thrust steering control functions instead of a pitch and yaw steering angle combination. In the NLP problem formulation, the three-direction cosines are parameterized by linear interpolation through a set of control nodes, which are included as SQP design variables. Because the magnitudes of the control nodes are unbounded, the thrust direction cosines $[\alpha_r, \alpha_\theta, \alpha_h]^T$ are normalized after linear interpolation so that the following necessary constraint is maintained:

$$\alpha_r^2 + \alpha_\theta^2 + \alpha_h^2 = 1 \tag{36}$$

Therefore, the NLP problem formulation involves 38 total SQP design variables: 11 control nodes for each thrust direction cosine (33 total variables), the initial LEO angles Ω_0 and θ_0, launch energy C_3, the ballistic coast time t_{coast}, and the powered capture time t_{capt}. Finally, the NLP problem involves two SQP equality constraints for the terminal state constraints (34) and one SQP inequality constraint for Eq. (35).

Results

Optimal trajectories are obtained for Earth–moon transfers using the Taurus launch vehicles outlined in Table 1 and the two EP thrusters shown in Table 2. Numerical integration of the transfer from LEO to circular lunar orbit is performed by a standard fourth-order, fixed-step, Runge–Kutta routine. The coasting ballistic trajectory and the powered lunar capture trajectory required 5000 and 2000 integration steps, respectively, for acceptable numerical accuracy.

Arcjet Thruster

The Taurus configuration with SRMs is utilized in conjunction with the arcjet thruster. The resulting optimal trajectory is presented in Fig. 1, which shows the projection of the transfer onto the x–y plane in an Earth-centered inertial frame. After burnout of the Taurus upper stage, the spacecraft has an energy (C_3) of −1.604 km^2/s^2 and an injected mass m_{TLI} of 396.0 kg. After a translunar coasting period of 3.17 days, the spacecraft passes within 9377 km of the lunar surface on a direct flyby, which increases the orbital energy of the trajectory. The spacecraft coasts for 22.9 more days, and the arcjet thruster is started past apogee, as indicated in Fig. 1. At the initiation of the powered capture, the spacecraft is $1.09(10^6)$ km from the lunar surface and $8.68(10^5)$ km above the Earth's surface. The powered lunar capture trajectory lasts 20.31 days, and the terminal circular lunar orbit is at an altitude of 30,184 km with an inclination of 87.7 deg, which is well within the lunar SOI radius of 66,300 km. Because the total trip time of the numerically

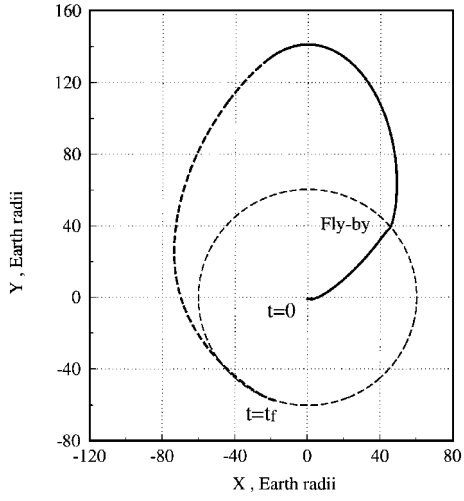

Fig. 1 Optimal lunar transfer, arcjet thruster: ——, coast; – – –, powered; and - - - -, moon orbit.

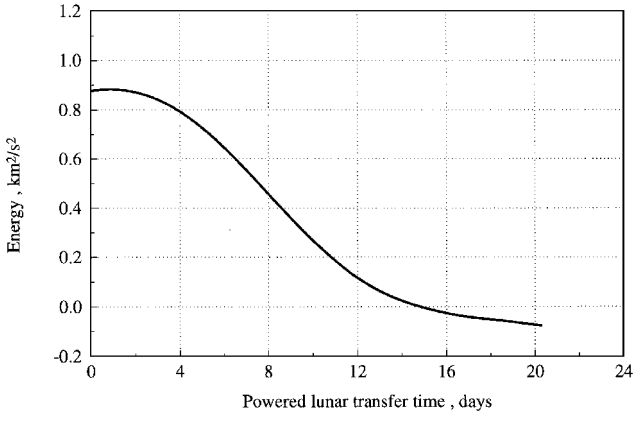

Fig. 2 Energy during powered lunar capture: arcjet thruster.

integrated trajectory is 46.4 days, the moon completes about 1.7 revolutions about the Earth, as demonstrated by Fig. 1. The remaining quasicircular transfer to the polar, 4000-km altitude lunar orbit as approximated by Edelbaum's[14] equations lasts 17.57 days and results in a final spacecraft mass in MLO of 310.0 kg and a mass ratio $m_{\mathrm{MLO}}/m_{\mathrm{TLI}}$ of 0.783. The total trip time to MLO is 64.0 days for this minimum-fuel transfer using chemical and EP stages, and the initial thrust-to-weight(T/W) ratio is $3.0(10^{-5})$. A comparable Earth–moon transfer at a similar T/W ratio using EP only requires a trip time of about 300 days.[19]

Recall that the direct optimization method attempts to maximize the final mass in MLO (m_{MLO}) and, therefore, the Edelbaum quasicircular transfer effects the performance index. Note that the lunar inclination at the end of the numerically simulated powered capture is very nearly polar so that very little fuel is expended on the plane-change maneuver during the quasicircular transfer to polar MLO.

The performance measure of the optimal trajectory may also be expressed in terms of the equivalent low-thrust velocity increment ΔV, which is calculated by using a variation of the rocket equation (27)

$$\Delta V = -c\ell_n(m_{\mathrm{MLO}}/m_{\mathrm{TLI}}) \tag{37}$$

Therefore, the optimal Earth–moon transfer to polar MLO using a Taurus launch vehicle with SRMs requires an equivalent low-thrust ΔV of 1080 m/s.

The two-body energy of the lunar capture trajectory is presented in Fig. 2 and is observed to be steadily decreasing. The optimal pitch and yaw thrust steering angles are presented in Fig. 3 and are derived from the resulting optimal thrust direction cosines $\alpha(t)$. Yaw angle is limited to ±90 deg and is measured from the instantaneous orbit plane to the thrust vector, and pitch angle is measured in the orbit plane from the local horizon to the projection of the thrust vector.

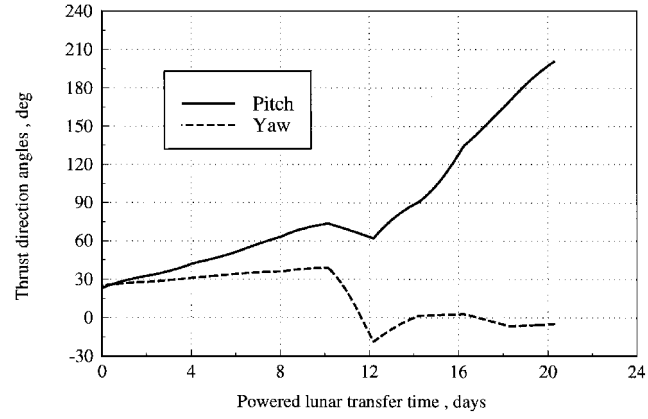

Fig. 3 Thrust direction angle histories: arcjet thruster.

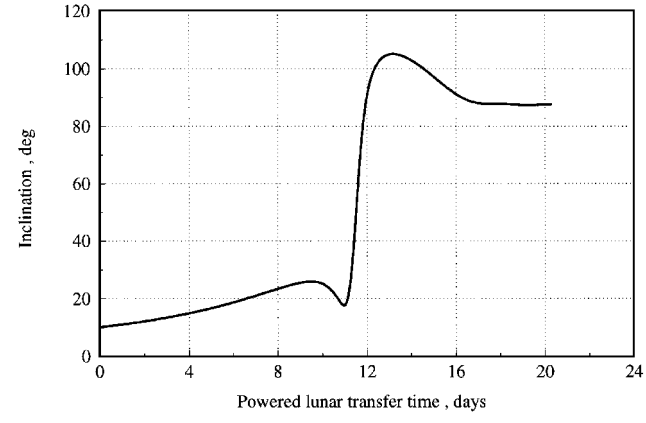

Fig. 4 Inclination during powered lunar capture: arcjet thruster.

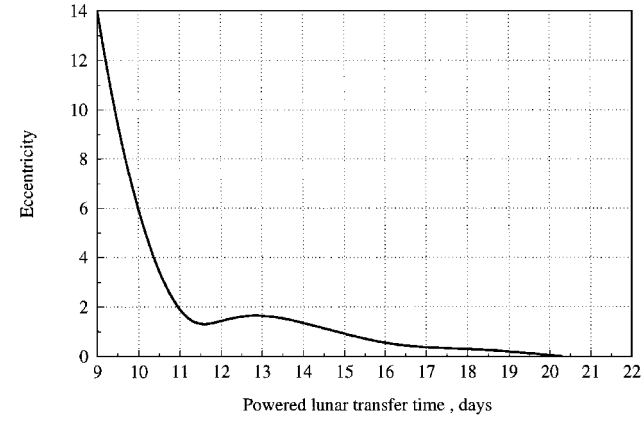

Fig. 5 Eccentricity during powered lunar capture: arcjet thruster.

Discontinuities in the thrust steering angles are due to the linear interpolation through the set of 11 control nodes per direction cosine. The optimal pitch and yaw steering are nearly linear until about 10 days into the powered capture. Between 10 and 14 days, the majority of the plane-change maneuver is accomplished, as demonstrated in Figs. 3 and 4. After 14 days, the thrust is nearly in-plane and continues to follow a nearly linear pitch steering profile, which ends with the thrust vector opposing the velocity vector as a circular orbit is established. Finally, the eccentricity history during the latter stages of the powered lunar capture trajectory is presented in Fig. 5.

SPT Thruster

The Taurus configuration without SRMs is used for the spacecraft with the SPT thruster. The optimal trajectory is presented in Fig. 6, which again shows the transfer in an Earth-centered inertial frame. Upon upper stage burnout, energy (C_3) is -2.016 km^2/s^2, and the injected mass m_{TLI} is 342.5 kg. After a translunar coast of 3.78 days, the spacecraft receives an energy boost as a result of a direct lunar

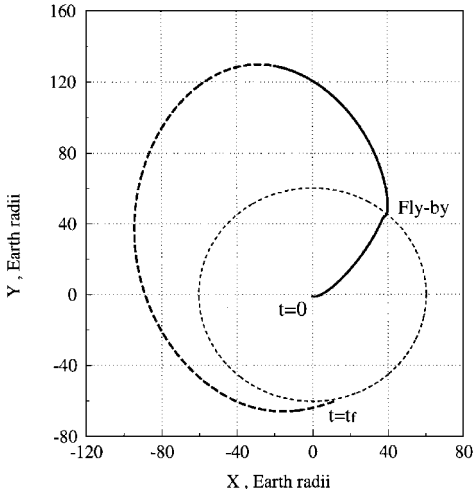

Fig. 6 Optimal lunar transfer, SPT thruster: ——, coast; – – –, powered; and - - - -, moon orbit.

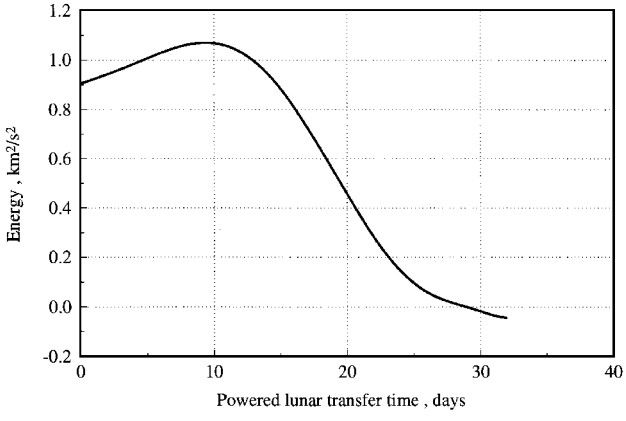

Fig. 7 Energy during powered lunar capture: SPT thruster.

flyby with a perilune altitude of 5909 km. The spacecraft coasts for an additional 12.79 days, at which time the SPT thruster is started just prior to apogee. At the initiation of the powered capture, the spacecraft is $1.09(10^6)$ km from the lunar surface and $8.42(10^5)$ km above the Earth's surface. The powered lunar capture trajectory lasts 31.95 days and the terminal circular lunar orbit is at an altitude of 53,126 km with an inclination of 84.1 deg. Therefore, the total trip time of the numerically integrated trajectory is 48.52 days, and the moon completes about 1.8 revolutions about the Earth, as demonstrated in Fig. 6. The remaining quasicircular transfer to polar MLO lasts 58.49 days and results in a final spacecraft mass in MLO of 322.1 kg ($m_{\mathrm{MLO}}/m_{\mathrm{TLI}} = 0.940$) and an equivalent low-thrust ΔV of 965 m/s, which is 115 m/s lower than the arcjet case. The total trip time is 107.0 days, and the initial T/W ratio is $1.2(10^{-5})$. Based on the results from Ref. 19, the trip time for an all-EP Earth–moon transfer with a similar T/W ratio is conservatively estimated to be over 550 days.

The higher I_{sp} for the SPT thruster results in a more efficient transfer compared to the arcjet case, and this is demonstrated by the reduced equivalent ΔV and the 12-kg increase in delivered mass. This is despite a Taurus launch vehicle configuration without SRMs, which results in an injected mass that is 53.5 kg lighter than the SRM option.

The two-body energy of the lunar capture trajectory is presented in Fig. 7, and the optimal pitch and yaw thrust steering angles are presented in Fig. 8. As before, the steering profile ends with the thrust vector opposing the velocity vector as a circular orbit is established. Again, the majority of the plane-change maneuver is performed in the latter stage of the capture trajectory, as demonstrated by the yaw steering angle in Fig. 8 and the corresponding inclination history in Fig. 9. The eccentricity history during the latter stage of the powered lunar capture trajectory is presented in Fig. 10.

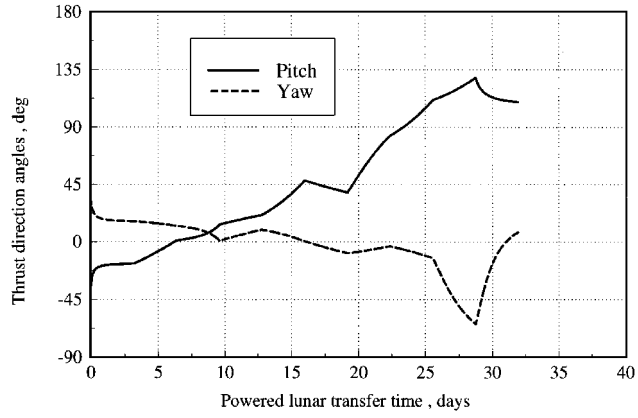

Fig. 8 Thrust direction angle histories: SPT thruster.

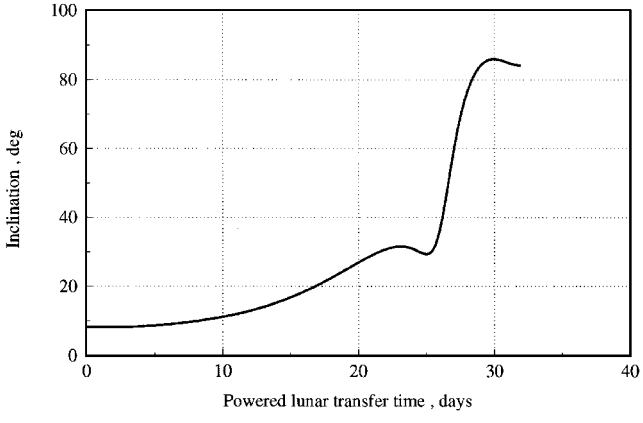

Fig. 9 Inclination during powered lunar capture: SPT thruster.

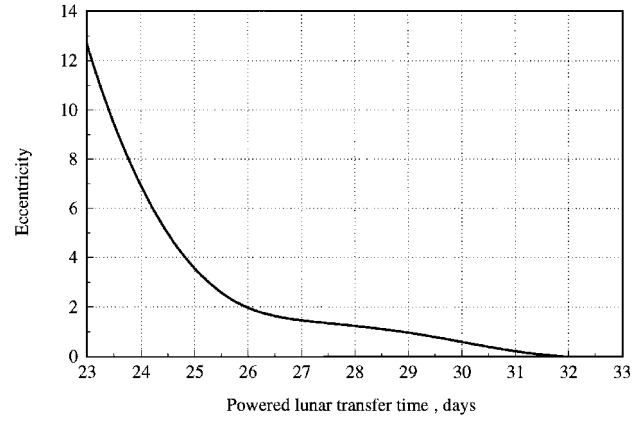

Fig. 10 Eccentricity during powered lunar capture: SPT thruster.

Conclusions

The feasibility of performing Earth–moon transfers using a combination of chemical and EP stages has been demonstrated by obtaining minimum-fuel, three-dimensional trajectories. The optimal control problem is replaced by a NLP problem, which in turn is solved by a constrained parameter optimization method. Both trajectory solutions exhibited an unpowered lunar flyby to provide a gravity assist followed by a continuous low-thrust capture to an inclined circular lunar orbit. It was found that very little propellant is expended for the plane change during the spiral transfer to the polar MLO because the powered lunar capture phase places the spacecraft in a nearly vertical plane with respect to the moon. Furthermore, the combined use of chemical and EP reduces the total trip time by a factor of five as compared to Earth–moon transfers using EP alone. This preliminary analysis demonstrates that a smaller sized launch vehicle (Taurus) in conjunction with current-term EP technology (arcjet and plasma thrusters) can deliver sufficient payloads for scientific exploration to polar lunar orbit. Future analyses should utilize a more accurate (noncircular) model of the Earth–moon system,

and because the lunar flyby results in a large apogee distance, the gravitational effects of the sun should probably be included. The preliminary results also suggest that the plasma thruster exhibits better payload performance compared to the arcjet thruster.

Appendix A: Position Vectors in the RTH Frame

The calculations of the Earth-spacecraft position vector $\boldsymbol{r}_1$ and the Earth–moon position vector $\boldsymbol{r}_{12}$ required for the computation of ∇U in Eq. (24) are presented in this section. These position vectors are in the moon-centered, inertial, orbit-plane RTH frame.

At the initiation of the powered moon-capture trajectory, the moon-centered inertial $+x$ axis points from the moon to the Earth with the x–y plane coincident with the Earth–moon orbit plane. If we define unit vectors $\boldsymbol{i}_x$, $\boldsymbol{i}_y$, and $\boldsymbol{i}_z$ along this moon-centered Cartesian frame, then the position vector $\hat{\boldsymbol{r}}_{21}$ from the moon to the Earth is

$$\hat{\boldsymbol{r}}_{21} = D\cos\omega\tau\boldsymbol{i}_x + D\sin\omega\tau\boldsymbol{i}_y \tag{A1}$$

where the caret indicates reference to the Cartesian frame. The variable τ is the powered capture time, and $\tau = 0$ indicates the start of the capture trajectory. The position vector $\hat{\boldsymbol{r}}_{12}$ from the Earth to the moon is, therefore,

$$\hat{\boldsymbol{r}}_{12} = -\hat{\boldsymbol{r}}_{21} \tag{A2}$$

Finally, the position vector $\boldsymbol{r}_{12}$ in the RTH frame is computed by using the coordinate transformation between the Cartesian frame and the rotating radial frame

$$\boldsymbol{r}_{12} = Q\hat{\boldsymbol{r}}_{12} \tag{A3}$$

where the rotation matrix Q is

$$Q = \begin{pmatrix} q_{11} & q_{12} & q_{13} \\ q_{21} & q_{22} & q_{23} \\ q_{31} & q_{32} & q_{33} \end{pmatrix} \tag{A4}$$

$$q_{11} = \cos\Omega\cos\theta - \sin\Omega\sin\theta\cos i$$

$$q_{12} = \sin\Omega\cos\theta + \cos\Omega\sin\theta\cos i \qquad q_{13} = \sin\theta\sin i$$

$$q_{21} = -\cos\Omega\sin\theta - \sin\Omega\cos\theta\cos i$$

$$q_{22} = -\sin\Omega\sin\theta + \cos\Omega\cos\theta\cos i \qquad q_{23} = \cos\theta\sin i$$

$$q_{31} = \sin\Omega\sin i \qquad q_{32} = -\cos\Omega\sin i \qquad q_{33} = \cos i$$

Once the $\boldsymbol{r}_{12}$ vector is computed in the RTH frame, the Earth-spacecraft vector $\boldsymbol{r}_1$ in the RTH frame is computed:

$$\boldsymbol{r}_1 = \boldsymbol{r}_{12} + \boldsymbol{r} \tag{A5}$$

where $\boldsymbol{r} = r\boldsymbol{i}_r$ is the spacecraft position vector in the moon-centered RTH frame.

Appendix B: Transforming the Boundary Conditions

In this Appendix, the transformation of the state at the end of the ballistic coast phase from the Earth-centered, rotating Cartesian frame to the moon-centered RTH frame is presented. The state at the end of the coast phase, as expressed in the Earth-centered rotating Cartesian frame, is $[x, y, z, u, v, w]^T$. Recall that the $+x$ axis of this rotating frame is always pointing from the Earth to the moon. Also recall that the $+x$ axis of the nonrotating moon-centered Cartesian frame is defined as pointing from the moon to the Earth at the instant the powered lunar capture phase is initiated (the $+z$ axis of both systems remains along the Earth–moon angular velocity vector). Therefore, the signs of x, y, u, and v must be reversed, and the position and velocity components in the moon-centered frame are

$$x_m = D - x \tag{B1}$$

$$y_m = -y \tag{B2}$$

$$z_m = z \tag{B3}$$

$$u_m = -u - \tilde{\omega}y_m \tag{B4}$$

$$v_m = -v + \tilde{\omega}x_m \tag{B5}$$

$$w_m = w \tag{B6}$$

where $[x_m, y_m, z_m, u_m, v_m, w_m]^T$ are the position and velocity components in the fixed moon-centered Cartesian frame. In this section, the Earth–moon rotation rate is denoted by $\tilde{\omega}$ to avoid confusion with argument of periapsis ω. The classical orbital elements $(a, e, i, \Omega, \omega, \nu)$ with respect to the moon can be obtained from $\boldsymbol{r} = [x_m, y_m, z_m]^T$ and $\boldsymbol{v} = [u_m, v_m, w_m]^T$ by defining the angular momentum vector $\boldsymbol{h}$, the nodal vector $\boldsymbol{n}$, and the eccentricity vector $\boldsymbol{e}$ (see Ref. 20 for details). Finally, the remaining elements of the state vector in the moon-centered RTH frame are computed from $\boldsymbol{r}$, $\boldsymbol{v}$, $\boldsymbol{h}$, and the orbital elements

$$r = \|\boldsymbol{r}\| \tag{B7}$$

$$v_\theta = \|\boldsymbol{h}\|/r \tag{B8}$$

$$v_r = \left(\|\boldsymbol{v}\|^2 - v_\theta^2\right)^{\frac{1}{2}} \tag{B9}$$

$$\theta = \omega + \nu \tag{B10}$$

where the radial velocity v_r has the same sign as the inner product $\boldsymbol{r}^T\boldsymbol{v}$.

References

[1] Tang, S., and Conway, B. A., "Optimization of Low-Thrust Interplanetary Trajectories Using Collocation and Nonlinear Programming," *Journal of Guidance, Control, and Dynamics*, Vol. 18, No. 3, 1995, pp. 599–604.

[2] Titus, N. A., "Optimal Station-Change Maneuver for Geostationary Satellites Using Constant Low Thrust," *Journal of Guidance, Control, and Dynamics*, Vol. 18, No. 5, 1995, pp. 1151–1155.

[3] Betts, J. T., "Optimal Interplanetary Orbit Transfers by Direct Transcription," *Journal of the Astronautical Sciences*, Vol. 42, No. 3, 1994, pp. 247–268.

[4] Sponable, J. M., and Penn, J. P., "Electric Propulsion for Orbit Transfer: A Case Study," *Journal of Propulsion and Power*, Vol. 5, No. 4, 1989, pp. 445–451.

[5] Burton, R. L., and Wassgren, C., "Time-Critical Low-Thrust Orbit Transfer Optimization," *Journal of Spacecraft and Rockets*, Vol. 29, No. 2, 1992, pp. 286–288.

[6] Oleson, S. R., Myers, R. M., Kluever, C. A., Riehl, J. P., and Curran, F. M., "Advanced Propulsion for Geostationary Orbit Insertion and North-South Station Keeping," AIAA Paper 95-2513, July 1995.

[7] Spitzer, A., "Near Optimal Transfer Orbit Trajectory Using Electric Propulsion," AAS Paper 95-215, Feb. 1995.

[8] Guelman, M., "Earth-to-Moon Transfer with a Limited Power Engine," *Journal of Guidance, Control, and Dynamics*, Vol. 18, No. 5, 1995, pp. 1133–1138.

[9] Golan, O. M., and Breakwell, J. V., "Minimum Fuel Lunar Trajectories for Low-Thrust Power-Limited Spacecraft," AIAA Paper 90-2975, Aug. 1990.

[10] Pierson, B. L., and Kluever, C. A., "Three-Stage Approach to Optimal Low-Thrust Earth–Moon Trajectories," *Journal of Guidance, Control, and Dynamics*, Vol. 17, No. 6, 1994, pp. 1275–1282.

[11] Kluever, C. A., and Pierson, B. L., "Optimal Low-Thrust Three-Dimensional Earth–Moon Trajectories," *Journal of Guidance, Control, and Dynamics*, Vol. 18, No. 4, 1995, pp. 830–837.

[12] Kluever, C. A., "Spacecraft Optimization with Combined Chemical–Electric Propulsion," *Journal of Spacecraft and Rockets*, Vol. 32, No. 2, 1995, pp. 378–380.

[13] Szebehely, V. G., *Theory of Orbits, the Restricted Problem of Three Bodies*, Academic, New York, 1967, pp. 7–21.

[14] Edelbaum, T. N., "Propulsion Requirements for Controllable Satellites," *ARS Journal*, Vol. 31, No. 8, 1961, pp. 1079–1089.

[15] Anon., "Commercial Taurus Launch System Payload User's Guide," Orbital Sciences Corp., Doc. TD-2493, Chantilly, VA, Aug. 1992.

[16] Janson, S. W., "The On-Orbit Role of Electric Propulsion," AIAA Paper 93-2220, July 1993.

[17] Pierson, B. L., "Sequential Quadratic Programming and Its Use in Optimal Control Model Comparisons," *Optimal Control Theory and Economic Analysis 3*, North-Holland, Amsterdam, 1988, pp. 175–193.

[18] Pouliot, M. R., "CONOPT2: A Rapidly Convergent Constrained Trajectory Optimization Program for TRAJEX," Convair Div., General Dynamics, GDC-SP-82-008, San Diego, CA, 1982.

[19] Kluever, C. A., and Chang, K.-R., "Electric-Propulsion Spacecraft Optimization for Lunar Missions," *Journal of Spacecraft and Rockets*, Vol. 33, No. 2, 1996, pp. 235–239.

[20] Bate, R. R, Mueller, D. D., and White, J. E., *Fundamentals of Astrodynamics*, Dover, New York, 1971, pp. 61–63.